Production of quarkonium states at the ATLAS experiment

V. Kartvelishvili (on behalf of the ATLAS collaboration)

Department of Physics, Lancaster University, LA1 4YB, United Kingdom

E-mail: v.kartvelishvili@lancaster.ac.uk

Abstract. An overview is given of recent measurements of the production of various heavy quarkonium states in pp collisions at $\sqrt{s} = 7$ TeV, using the ATLAS detector at the LHC. These include the production cross sections of the C-even states χ_{c1} and χ_{c2} in their radiative decay modes into $J/\psi\gamma$, and of the radially excited vector state $\psi(2S)$ in its decay mode into $J/\psi\pi^+\pi^-$. Differential spectra in transverse momentum are measured separately for promptly produced charmonium states, originating from QCD sources, and for non-prompt states from the decays of B-hadrons. Results are compared to other existing measurements and various theoretical models.

1. Introduction

Almost 40 years after the discovery of the J/ψ meson, the investigation of hidden heavy flavour production processes in hadronic collisions still presents significant challenges to both theory and experiment. Large amounts of LHC data have now become available, thus opening a new energy frontier and a new chapter in such studies.

This note is an overview of recent results on quarkonium production from the ATLAS collaboration [1] at the LHC, based on the data collected at the c.m. energy of 7 TeV.

2. $\psi(2S)$ production

The production of the $\psi(2S)$ meson was studied in its decay mode into $J/\psi\pi^+\pi^-$ [2]. The J/ψ candidates, triggered by a low-p_T dimuon trigger, were combined offline with two oppositely charged tracks to form $\psi(2S)$ candidates. A kinematic fit constraining the two muon tracks to the J/ψ mass and all four tracks to a common vertex was used to improve resolution, both for the invariant mass of the candidates and the (pseudo-) proper decay time of the vertex. The $\psi(2S)$ candidates were divided into 30 analysis bins (3 in rapidity and 10 in transverse momentum). Candidates were weighted using acceptance and efficiency maps, derived using a combination of Monte Carlo and data-driven methods, and a 2D mass-lifetime unbinned maximum-likelihood fit was performed to extract the production cross section in each of the analysis bins. Fig. 1 shows mass and lifetime projections for a sample analysis bin, illustrating the mass resolution, and the separation of the $\psi(2S)$ signal into prompt and non-prompt components.

The measured fraction of non-prompt $\psi(2S)$ mesons (produced from long-lived sources such as b-hadron decays) is shown in Fig. 2. The fraction increases with increasing p_T, reaching about 70% at 100 GeV across the whole rapidity range studied here.

Journal of Physics: Conference Series **556** (2014) 012011 doi:10.1088/1742-6596/556/1/012011

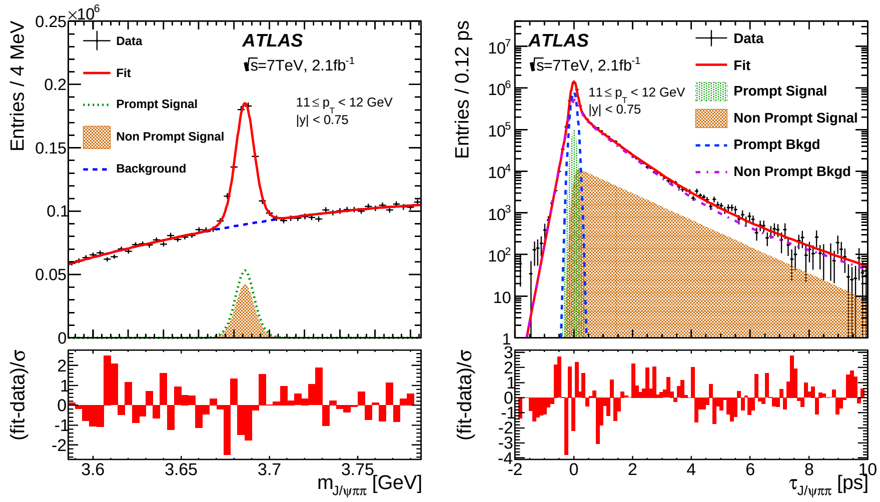

Figure 1. Mass and lifetime projections for the $\psi(2S)$ candidates from a sample analysis bin.

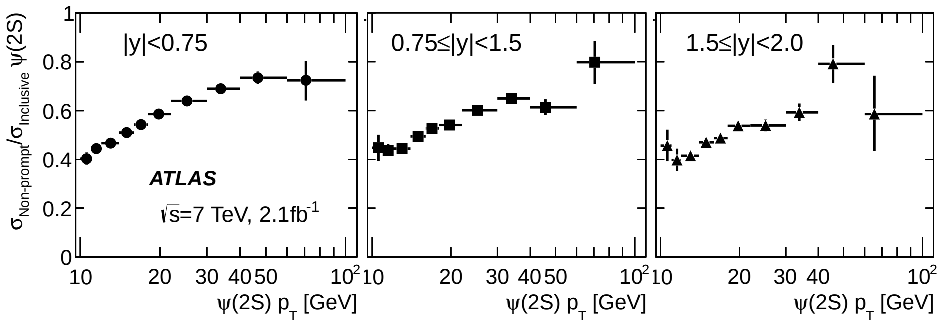

Figure 2. The measured fraction of non-prompt $\psi(2S)$ mesons.

The measured differential cross sections are shown in Fig. 3, separately for prompt and non-prompt $\psi(2S)$ mesons. Comparison with various theoretical models shows that NLO NRQCD and FONLL are doing a good job in describing data; more details can be found in [2].

3. χ_c production

The production the of C-even charmonium states χ_{c1} and χ_{c2} was studied in their radiative decay mode into $J/\psi\gamma$ [3]. As in the $\psi(2S)$ case, the J/ψ candidates were triggered by a low-p_T dimuon trigger and were combined offline with photon candidates. In order to achieve the best mass resolution, the analysis was confined to the central rapidity region, using the photons converted into e^+e^- pairs. The left plot in Fig. 4 shows the invariant mass distribution of all selected $\mu^+\mu^-\gamma$ candidates, where separate peaks from various χ_c states are clearly visible, while the right plot presents the lifetime distribution, used to separate the χ_c signal into prompt and non-prompt contributions.

The $\mu^+\mu^-\gamma$ candidates were weighted using acceptance and efficiency maps derived using a combination of Monte Carlo and data-driven methods, and a 2D mass-lifetime unbinned maximum-likelihood fit was performed to extract the production cross section in each of the five bins in transverse momentum, separately for prompt and non-prompt production.

The differential cross sections of promptly produced χ_{c1} and χ_{c2} states are shown in Fig. 5,

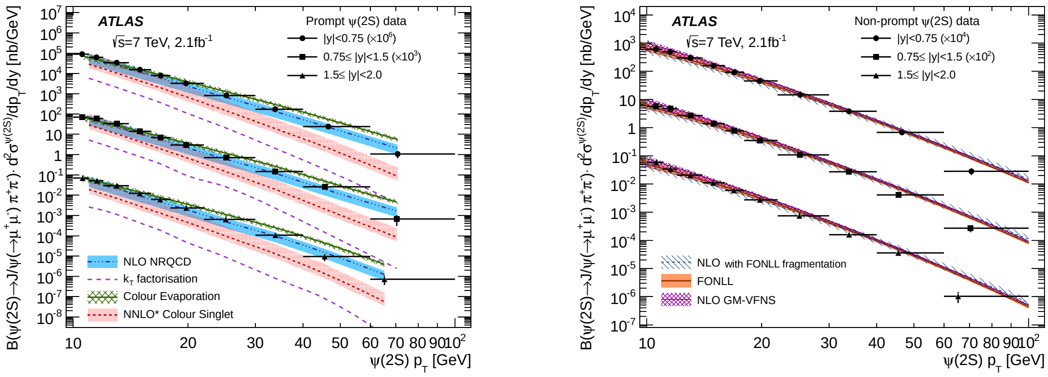

Figure 3. Measured differential cross-sections for prompt (left) and non-prompt (right) $\psi(2S)$ production, in comparison with theoretical predictions (see [2] for more details).

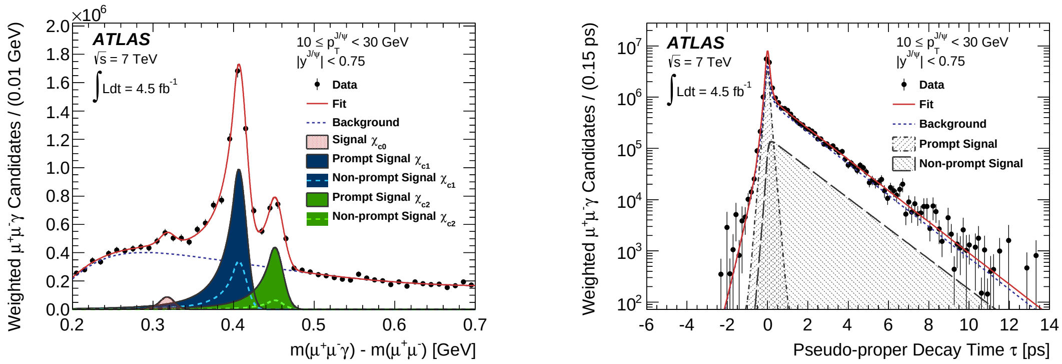

Figure 4. Mass (left) and lifetime (right) distributions of all selected $\mu^+\mu^-\gamma$ candidates.

while non-prompt production cross sections are presented in Fig. 6. Both are compared with

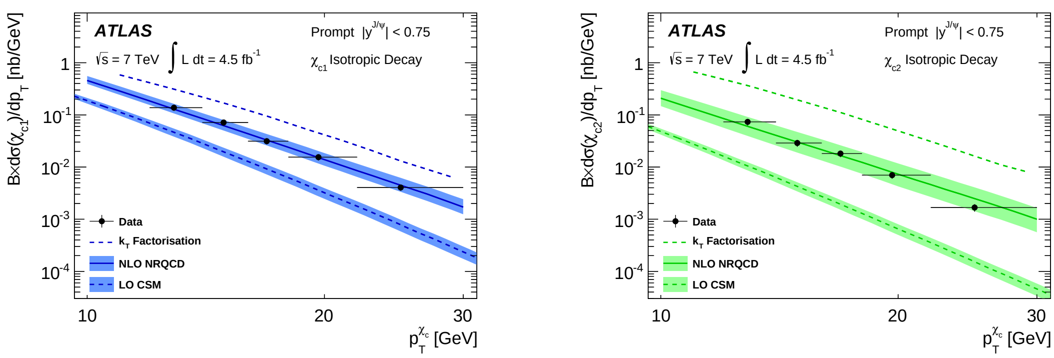

Figure 5. Differential cross sections for prompt production of χ_{c1} (left) and χ_{c2} (right).

various theoretical models (see [3] for details).

While trying to understand the dynamics of charmonium production, it is important to know what fraction of prompt J/ψ is produced from χ_c feed-down. These results, shown in Fig. 7, are in good agreement with predictions of NLO NRQCD.

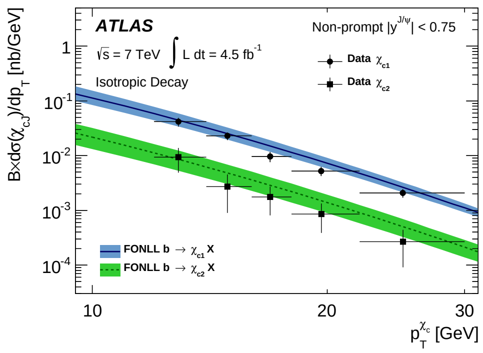

Figure 6. Differential cross sections for non-prompt production of χ_{c1} and χ_{c2}.

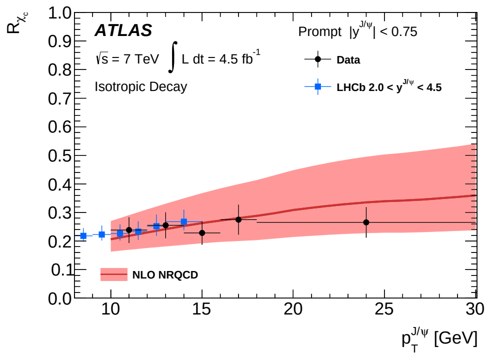

Figure 7. Fraction of J/ψ mesons produced from χ_c feed-down.

With the same data selection, ATLAS also measured the branching ratio of the decay $B^{\pm} \to \chi_{c1} K^{\pm}$, using the decay $B^{\pm} \to J/\psi K^{\pm}$ as a control mode. The mass spectrum of $B^{\pm} \to \chi_{c1} K^{\pm}$ candidates is shown in Fig. 8. The measured branching ratio, presented in Fig. 9,

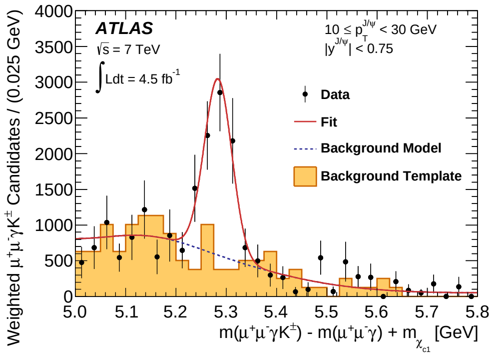

Figure 8. Invariant mass spectrum of $B^{\pm} \to \chi_{c1} K^{\pm}$ decay candidates.

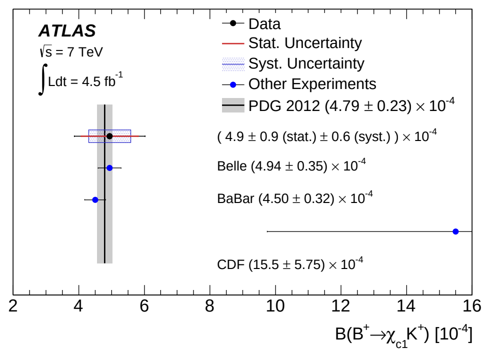

Figure 9. Branching ratio measurements for $B^{\pm} \to \chi_{c1} K^{\pm}$ decay.

is consistent with the best B-factory results and shows a significant improvement on the previous hadron collider measurement, with a great promise for Run II.

4. Summary

With the excellent performance of the LHC and ATLAS in Run I, new insights into the dynamics of quarkonium production in hadronic collisions have become possible. Ever wider variety and range of kinematic variables are being explored, thus providing new areas where the experimental measurements confront theoretical predictions.

More quarkonium-related results from ATLAS are covered in contributions from E. Bouhova-Thacker and M. Watson elsewhere in these proceedings.

References

[1] ATLAS collaboration, *JINST* **3** (2008) S08003.
[2] ATLAS collaboration, CERN-PH-EP-2014-095, *JHEP* (to be published), arXiv:1407.5532 [hep-ex].
[3] ATLAS collaboration, *JHEP* **07** (2014) 154, arXiv:1404.7035 [hep-ex].